Nonlinear Stability Analysis for Artificial Kidney Multi-compartmental Models

Rammah Abohtyra[1] CV Hollot, Fellow, IEEE, J Horowitz, Yossi Chait

***Index Terms*—Artificial kidney, Hemodialysis, Ultrafiltration, Nonlinear Stability, Invariant slope.**

***Abstract*—This paper investigates the global stability of artificial kidney fluid volume dynamics described by a nonlinear multi-compartment model of extracellular fluid volume exchange during dialysis. Only a few papers in the literature have addressed the stability of similar classes of compartment models. In these papers, the global stability of such models is established using the Lyapunov method; however, their results are not applicable to our model. We developed a new nonlinear Lyapunov function which enables us to prove the stability of a general class of nonlinear multi-compartment models. To examine the oscillatory behavior of the model under external input, we tested our stability results during the short-term of the ultrafiltration process.**

I. Introduction

Patient in end-stage kidney disease are often suffering from multiple acid-base derangements and fluid shift complications [8], [22]. Artificial kidney (hemodialysis) is a life-saving therapy that corrects acid-base derangement and removes fluid accumulation [21], [26], [18]. During artificial kidney treatment, fluid is removed from the plasma pool by ultrafiltration (UFR) leading to fluid refilling from the interstitial compartment to overcome the fluid shift [24], [23]. An adequate balance between fluid removal and refill is associated with increased morbidity and mortality risk [25].

The total body fluid is distributed mainly between two compartments, the extracellular compartment (ECC), which contains fluid outside the cells including interstitial fluid and plasma (about 20% of the body weight), and the intracellular compartment (ICC) which contains fluid inside the cells, (about 40% of the body weight) [11]. The ECC is divided by a capillary membrane into the interstitial compartment and the intravascular compartment. The intravascular compartment contains blood which consists of cells (e.g., red blood cells) and plasma. The plasma is the noncellular part of the blood [7], [13]. Fluid-exchange between the intravascular and interstitial compartments is controlled by the Starling forces, namely, the osmotic and hydrostatic pressure gradients [4], [6]. If the difference between these gradients is negative, there will be a fluid filtration across the capillary membrane into the intravascular compartment. However, if the difference is positive, resulting in a filtration of fluid into the interstitial spaces.

Over the past years, there has been an active research effort to characterize fluid removal from the intravascular compartment by UF and vascular refilling from the interstitial spaces during hemodialysis (HD). Two-compartment models describing the short-term dynamics of vascular refilling and UF have been derived in (e.g.,[2], [4], [15], [27], [28]). For example, in [4], the authors provided a simplified linear two-compartment model and nonlinear two-compartment model incorporating the lymphatic system. This work addresses the contribution of lymph flow to the fluid movement from interstitial spaces to the intravascular compartment. More recently, in [2], the authors developed a nonlinear two-compartment model describing the vascular refilling during HD. This model considers (microvascular) fluid shifts between the compartments and lymph flow from the interstitial to the intravascular compartment.

Stability is an important requirement for fluid-exchange in the body and has not been addressed yet. There are many methods for analyzing stability of nonlinear models. Among them, we focus on Lyapunov stability approach. Exploring stability of nonlinear compartment model with Lyapunov method is a challenging task because it often requires searching for Lyapunov candidate by trial-and-error. Stability of a class of nonlinear compartment models, based on the Lyapunov approach, has been investigated in [3], [12], [14], [20]. Since the fluid flow of our model is non-positive, the results of these papers cannot be applied to our model because of the particular class of models under consideration.

A class of nonlinear compartment model, similar to our model, has been discussed in [19]. Sufficient conditions concerning the flows between the compartments are made (positive flow). These results, however, do not seem to be applicable to our model because the conditions are not satisfied, and the Lyapunov functions used are inappropriate for our model. In addition, another class of nonlinear models has been studied in [5]. Although these models have a similar structure to ours, the result of [5] is not applicable here because it pertains only to isolated equilibrium points.

Our contribution in this paper is as follows. We overcome these limitations, and provide a Lyapunov function to explore the nonlinear stability of a general class of nonlinear compartment model whose flow functions are non-positive and apply the result to the two-compartment model which describes the dynamics of fluid-exchange between the interstitial and intravascular compartments. To examine the behavior of the model under nonzero input, we tested the model during ultrafiltration process, using a specific profile.

We organize the paper as follows: We begin by defining the two main fluid compartments. In Section II, a brief description of the fluid-exchange of artificial kidney model is presented and an equilibrium set is computed. In Section III, stability analysis is provided including the main result. In Section IV, simulation examples are provided. Finally, in Section V is the

conclusion.

II. Artificial Kidney Model description

The two-compartment model represented by Fig. 1 is comprised of the intravascular and interstitial compartments, which are separated by a capillary membrane wall, and lymphatic flow returns a small amount of fluid from the interstitial compartment into the intravascular compartment [10]. Our model includes ultrafiltration (UF) term describing fluid removal from the intravascular compartment during HD treatment [2]. Because the plasma is the extracellular fluid part of the blood contained in the intravascular compartment, in this paper, we consider that the plasma volume is part of the intravascular compartment volume. There is a continuous microvascular fluid filtration between the intravascular and interstitial compartments via the capillary membrane.

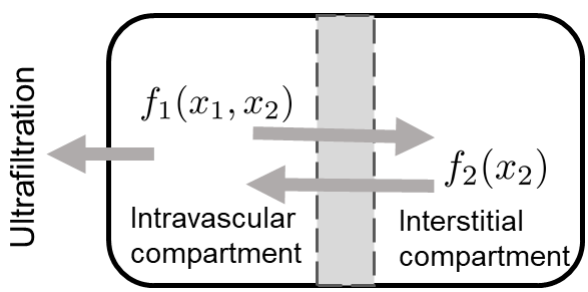

Figure 1. Two-compartment model used for the artificial kidney treatment, describing fluid-exchange between interstitium and intravascular compartment separated by a capillary membrane, and including lymph flow and UF.

The rate at which intravascular and interstitial volumes change in time is given by

$$\begin{aligned} \dot{x}_1 &= - f_1(x_1, x_2) + f_2(x_2) - u \\ \dot{x}_2 &= f_1(x_1, x_2) - f_2(x_2) \end{aligned} \tag{1}$$

where $x = (x_1, x_2)$ is the fluid volume state of the model, x_1 and x_2 represent the intravascular and interstitial volume, respectively, $f_1(x)$ denotes the flow of the fluid filtration between two-compartments across the capillary membrane which is governed by the Starling's equation [2], $f_2(x_2)$ describes the lymphatic flow, and u denotes the ultrafiltration rate (UFR). The mathematical description of these functions is given in the Appendix.

The hematocrit, Hct, is a percentage of blood volume $(V_{rbc} + x_1)$, which depends on both the volume of red blood cells (RBCs) and intravascular fluid volume x_1. Changing x_1 can change the hematocrit without a change in the number of RBCs. The Hct is given by

$$Hct(t) = \frac{V_{rbc}}{V_{rbc} + x_1(t)} \tag{2}$$

Note that the nonlinear functions $f_1(x)$ and $f_2(x_2)$ in (12) and (16), respectively, are not continuous in the entire domain of $x \in \mathbb{R}^2$. This readily can be seen from (15), in words at the origin. A brief description is provided in the Appendix about how we specified this subset.

III. Stability Analysis

The class of nonlinear compartment models that we are dealing with in this paper is developed in [3], [19], [20], whose fluid flow is non-positive. In order to derive a general stability result (Theorem 1 below) for this class, we consider n compartments where the dynamics of a certain material of interest in the ith compartment at time t, denoted by $x_i(t)$, is given by

$$\dot{x}_i(t) = -a_{ii} f_i(x_i(t)) + \sum_{j \neq i} a_{ij} f_j(x_j(t)) + u_i \tag{3}$$

where $a_{ij} \geq 0$, $i, j \in \{1, \ldots, n\}$. Therefore, a real matrix satisfying these conditions is called compartment matrix [19]. In a more compact form, this dynamics can be written as

$$\dot{x} = Af(x) + u, \quad x_0 \neq 0 \tag{4}$$

where the matrix $A \in \mathbb{R}^{n \times n}$ is (symmetric matrix) defined by

$$A = \begin{bmatrix} -a_{11} & a_{12} & \cdots & a_{1n} \\ a_{21} & -a_{22} & \cdots & a_{2n} \\ \vdots & \ddots & \ddots & \vdots \\ a_{n1} & \cdots & a_{n,n-1} & -a_{nn} \end{bmatrix}$$

It is possible to rearrange (1) in the form of (4). This rearrangement is explicitly derived in the Appendix B.

As in [19], equation (1) can be written in a compact form

$$\dot{x} = Ag(x) + u, \quad x_0 \neq 0 \tag{5}$$

where $g(x) = [\ g_1(x_1) \quad g_2(x_2)\ ]^T$ and A is symmetric, negative semi-definite where

$$A = \begin{bmatrix} -1 & 1 \\ 1 & -1 \end{bmatrix}.$$

A. Equilibrium Set

To obtain the equilibrium point x_{eq}, we assume that there is no UFR ($u = 0$). At equilibrium, we have

$$0 = Ag(x_{eq}) \tag{6}$$

Due to high nonlinearity in (5), we could not derive an explicit expression, analytically, for the equilibrium point, x_{eq},, however, we compute instead an equilibrium set $\mathcal{E}$, numerically, by defining x_1 and x_2 which satisfy the following relation

$$g_1(x_1) = g_2(x_2)$$

where this equality occurs at equilibrium (6).

Using the previous relation, it appears that the lower value of x_1 is 0.7 at which $x_2 = 6.61$. This means that for smaller values of x_1 than 0.7, the corresponding value of x_2, which satisfy the previous relation, will be less that 6.61 where $g(x)$ is discontinuous. Since, the fluid volume of the intravasculat compartment is about 4-5 Liters in a healthy, 70 Kg man, and the fluid volume in the interstitial compartment is about 28 liters [6], in this paper, we assume that the maximum amount of fluid volume in the intravascular and interstitial compartments are 4, 30 Liters, respectively. We specify a restrictive domain as follows by this subset

$$B := \{x \in \mathbb{R}^2 \mid 4 \geq x_1 \geq 0.7 \text{ and } 30 \geq x_2 \geq 6.61\} \tag{7}$$

This closed subset starts at (0.7, 6.61) liters and closed at (4, 30) liters, which is illustrated by Fig. 2.

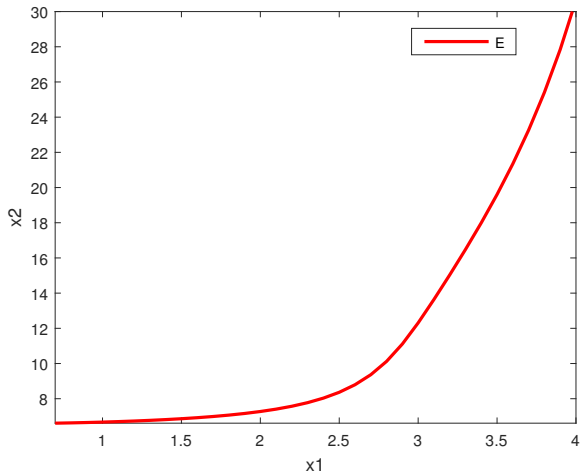

Figure 2. The equilibrium set of the model (5) for $x \in B$, using the Phase-plane plot.

We define the equilibrium set for the model in (5) as follows.

Definition 1. Consider model (5) with $u = 0$, the equilibrium set of (5) is define by

$$E := \{x \in B \mid Ag(x) = 0\}$$

in which $g_1(x_1) = g_2(x_2)$.

IV. Results

We will establish the stability result of the general compartment model in (4). We will invoke LaSalle's Theorem since it is applicable to system having an equilibrium set rather than an isolated equilibrium point [16]. The main result of this paper is given in the next two theorems. The fluid volume in each compartment has a dynamics defined in (1). This dynamics can be determined by a certain slope s. When $u \equiv 0$ in (5), the slope is given very simply as follows:

$$s = \frac{\dot{x}_2}{\dot{x}_1} \tag{8}$$

Lemma 2. *When $u_1 \equiv 0$ in (5), the slope $s = -1$ for all $x \in B - E$.*

Proof: We substitute (5) into (8), thus

$$s = -\frac{g_1(x_1) + g_2(x_2)}{g_1(x_1) - g_2(x_2)} = -1, \forall x \in B - E$$

■

Note that for all points in E, by definition $\dot{x}_1 = 0$, $\dot{x}_2 = 0$, consequently, the slope is undefined. In the next section, we will derive the main result of this paper in Theorem 3 and Theorem 4, which demonstrate nonlinear stability of a very general class of compartment models and study the stability under external input (ultrafiltration), followed by an application to the proposed extracellular two-compartment model.

Theorem 3. *Consider (4) with $u \equiv 0$ and let $\Omega \subset \mathbb{R}^n$ be compact and positively invariant with respect to the system in (4). Assume $f(x)$ is differentiable in Ω, and let E be the equilibrium set $E = \{x \in \Omega \mid Af(x) = 0\}$, and let $\frac{\partial f_i(x_i)}{\partial x_i} > 0$, $i = 1, \ldots, n$, $\forall x \in \Omega$. If $x_0 \in \Omega$, then $x(t)$ approaches E as $t \to \infty$.*

Proof: Consider the Lyapunov function candidate: $V(x) : \mathbb{R}^n \to \mathbb{R}$ defined by

$$V(x) = -\frac{1}{2} f(x)^T A f(x) \tag{9}$$

where this function is continuous, differentiable. The derivative of $V(x)$ with respect to the time is derived in the Appendix C as

$$\dot{V}(x) = -\sum_{i=1}^{n} \dot{x}_i^2 \frac{\partial f_i(x_i)}{\partial x_i} \tag{10}$$

where $\dot{x}_i$ is defined in (3). This function satisfies the following conditions:

- $\dot{V}(x) \leq 0, \forall x \in \Omega$,
- $\dot{V}(x) = 0, \forall x \in E$.

In fact, E is the largest invariant subset in which $\dot{V}(x) = 0$, this can be shown as follows. Obviously E is a subset of $\{x \in E \mid \dot{V}(x) = 0\}$. Now suppose x is such that $\dot{V}(x) = 0$. Then by (10) $\dot{x}_i = \dot{V}(x) = 0$ for all i, therefore, $x \in E$. It follow by LaSalle's Theorem (Theorem 4.4 in [29]), that $x(t)$ converges to E. ■

In the next subsection, we will invoke Theorem 3 to prove global stability of the fluid volume two-compartment model.

A. Application to Two-compartment Model

We will demonstrate the attractivity of the equilibrium set of the two-compartment model which defined in (5). To invoke Theorem 3, we consider model (4) with $n = 2$. For this model, the $\frac{\partial f_i(x_i)}{\partial x_i} > 0$, $i = 1, 2$, $\forall x \in B$ (see the Appendix) for all choices of the parameters having the same signs as those in (Table I). Consider the Lyapunov function:

$$V(x) = -\frac{1}{2} g(x)^T A g(x)$$

where in this case, matrix A is as defined in (5). Then

$$\dot{V}(x) = -\sum_{i=1}^{n=2} \dot{x}_i^2 \frac{\partial g_i(x_i)}{\partial x_i}$$

where $\dot{x}_i$, $i = 1, 2$ are given in (1). We simplify $\dot{V}$ as

$$\begin{aligned}
\dot{V}(x) &= -\dot{x}_1^2 \frac{\partial g_1(x_1)}{\partial x_1} - \dot{x}_2^2 \frac{\partial g_2(x_2)}{\partial x_2} \text{ where } (\dot{x}_2 = -\dot{x}_1) \\
&= -\dot{x}_1^2 \frac{\partial g_1(x_1)}{\partial x_1} - (-\dot{x}_1)^2 \frac{\partial g_2(x_{12})}{\partial x_2} \\
&= -\dot{x}_1^2 \frac{\partial g_1(x_1)}{\partial x_1} - \dot{x}_1^2 \frac{\partial g_2(x_2)}{\partial x_2}, \text{ which yield to} \\
\dot{V}(x) &= -\dot{x}_1^2 \left(\frac{\partial g_1(x_1)}{\partial x_1} + \frac{\partial g_2(x_2)}{\partial x_2} \right) \leq 0, \forall x \in B
\end{aligned}$$

By construction the subset B is a compact set. To show that B is a positively invariant set with respect to model (5), from (Lemma 2) if $x_0 \in B$, then $x(t)$ approaches E as $t \to \infty$ with a particular slope and direction such that $x(t)$ never leave B.

B. Stability Under Ultrafiltration

To explore the stability of the model under ultrafiltration, as an external input u, we use a specific class of ultrafiltration profile developed here [1] with the model. We show that the solution of the model x under u is not oscillatory and follows a closed trajectory contained in a pre-determined subset of the set B, and then x converges back to E when $u = 0$.

To show this, in (5), we let $Q(x) = -g_1(x_1) + g_2(x_2)$, and $Q_{x_1} = \frac{\partial Q(x)}{\partial x_1}$ and $Q_{x_2} = \frac{\partial Q(x)}{\partial x_2}$, (see Appendix D).

Theorem 4. *Consider (5) with $x_0 \in E$. Let $E^+ := \{x : Q(x) = 0\}$. Suppose Q is continuous on the interior of the 1st quadrant and satisfies the following:*

1) $Q_{x_1} < 0$, $\forall x \in E \cup E^+$.
2) $Q_{x_2} > 0$, $\forall x \in E \cup E^+$.

For given: $0 < u_{max} < \frac{\|x_0\|_1}{t_f}$, $\hat{u}(t) \geq 0$, and $t_f > 0$, take

$$u(t) \begin{cases} u_{max}, & 0 < t \leq t^* \\ \hat{u}(t) \leq u_{max}, & t^* < t \leq t_f \\ 0 & t > t_f. \end{cases} \tag{11}$$

Let $x(t)$ be a solution to (5) and let S be:

$S := \{x : 0 \leq Q(x) \leq u_{max}, x_1 \leq x_{10}, x_2 \leq x_{20}$, *and* $(x_1+x_2) > (x_{10}+x_{02}) - (u_{max}t^* + \int_{\hat{u}(t^*)}^{\hat{u}(t_f)} \hat{u}(s)ds)\}$.

Then $x(t) \in S$ for all $0 \leq t \leq t_f$.

The prove is provided in the Appendix E.

We will illustrate this result by considering the following numerical example.

V. Simulation Example

To test our results, we consider the model in (5) with three different initial conditions located as shown in Fig. 3. The initial volume (2,11) L, is chosen such that $Q(x) > 0$, ($Q(x) = -g_1(x_1) + g_2(x_2)$), whereas, the initial condition (3,6.61) is chosen at which $Q(x) < 0$. By simulation, the state x moves towards E with a slope equal to -1, in both cases, as shown in Fig. 3. However, when the model starts with initial condition on E, then x does not move, it stays at the same point on E for $t \geq 0$.

To investigate whether or not the solution of the model oscillates under an external input, we use a time varying ultrafiltration profile designed using the approach developed in [1]. This profile was designed to achieve a dialysis prescription which is to remove 3.78 L with a specified dialysis time of 3hrs 50 min. The designed time varying ultrafiltration input $u(t)$ is presented in Fig. 3.

We illustrate the behavior of the model under $u(t)$ in Fig. 4 , by a Phase-plane. The state of the model moves within a closed subset, during the time $0 < t \leq t_f$ where t_f = 3hrs 50 min. We prove these results only for patient dependent ultrafiltration profiles, however, we cannot grantee the same results for other type of ultrafiltration profiles.

VI. Conclusion

Since stability of fluid volume in the extracellular compartment is a significant element in fluid-exchange in the artificial kidney, this paper proposed a new stability approach to illustrate nonlinear stability of fluid volume of two-compartment model that describes the dynamics of fluid exchange between the intravascular and interstitial compartments. An equilibrium set to describe the fluid volume of the model at equilibrium is computed. Lyapunov function candidate is chosen correctly and LaSalle's Theorem is considered to illustrate the nonlinear stability of a general form of nonlinear compartment model. This result is then effectively used to investigate the stability of the fluid volume two-compartment model proposed in this paper. This function is able to insure the attactivity of the equilibrium set of the general model and obtain the same result for the two-compartment model.

We proved that the solution of the compartment model is stable and nonperiodic solution under specific type of ultrafiltration inputs. An example has been constructed to show that the solution of the model remains in a closed set during the dialysis treatment and then converged to as equilibrium volume after ultrafiltration.

Appendix

A. Model Description:

The flow $f_1(x)$:

$$f_1(x) = K_f(\Delta_p(t) - \Delta_\pi(t)) \tag{12}$$

where Δ_p and Δ_π represent the hydrostatic and osmotic pressure gradients, respectively, defined by

$$\Delta_p(t) = (P_c(t) - P_i(t)) \text{ and } \Delta_\pi(t) = (\pi_p(t) - \pi_i(t))$$

where P_c, P_i are the hydrostatic capillary and interstitial pressures, respectively at a given time t. Capillary pressure is described by

$$P_c(t) = P_v(t) + P_{off}$$
$$P_v(t) = d\left(100\frac{V_{rbc} + x_1(t)}{V_{rbc} + V_{P,eu}} + e\right)^l \tag{13}$$

where P_v is the venous pressure, P_{off} is a pressure offset, $x_1(t)$ is the intravascular volume at a given time t, V_{rbc} is the volume of red blood cells, $V_{P,eu}$ is intravascular volume at the euhydrated state, d, e and l are constants [9]. We define

$$P_i(t) = a\left(100\frac{x_2(t)}{V_{i,eu}}\right) + \frac{b}{\left(100\frac{x_2(t)}{V_{i,eu}} + c\right)} \tag{14}$$

where $x_2(t)$ represents interstitial fluid volume at a given time t, $V_{i,eu}$ refers to interstitial volume at the euhydrated state, a, b and c are constants [9]. However, π_p, π_i are the plasma and interstitial colloid osmotic pressures, respectively, at a given time t, given by

$$\begin{aligned} \pi_p(t) =& \frac{k_1 m_p}{x_1(t)} + \frac{k_2 m_p}{x_1^2(t)} + \frac{k_3 m_p}{x_1^3(t)} \\ \pi_i(t) =& \frac{k_1 m_p}{x_2(t)} + \frac{k_2 m_p}{x_2^2(t)} + \frac{k_3 m_p}{x_2^3(t)} \end{aligned} \tag{15}$$

where m_p and m_i describe the protein mass in plasma and interstitial volumes, respectively, k_1, k_2 and k_3 are constants

[17], and K_f is the capillary filtration coefficient obtained in [9].

$$f_2(x_2) = g\tanh(hP_i(t)) + i \tag{16}$$

where g, h, and i are constants [9]. During the fluid circulation between the two compartments, $f_2(x_2)$ is smaller that $f_1(x)$ [10]. Since x_1 and x_2 represent volume, they should be positive. Hence, we will restrict the domain of x_1 and x_2 over this range $x_1 > 0$, $x_2 > 0$. Therefore, we set the term inside the bracket $(\cdot)$ in (13) to be greater than zero, then we solve for x_1 accordingly. We repeat this step for the denominator in (14) to solve for x_2. Note that the constants in (Table I and II) are used here. As a result, $f_1(x)$ and $f_2(x)$ are continuous in the following restricted domain:$x_1 \geq 0.1$ and $x_2 \geq 6.61$.

B. Compartmental Model Arrangement

We use the model in (1) to transformer it into the compartment from (3):

$$\begin{aligned}\dot{x}_1 &= -f_1(x_1, x_2) + f_2(x_2) - u \\ &= -K_f(\triangle_p - \triangle_\pi) + f_2(x_2) - u \\ &= -K_f((P_c - Pi) - (\pi_p - \pi_i)) + f_2(x_2) - u\end{aligned} \tag{17}$$

By collecting terms of x_1 and x_2 into two groups, yields

$$\begin{aligned}\dot{x}_1 &= -K_f((P_c - \pi_p) - (Pi - \pi_i)) + f2(x_2) \\ &= -\underbrace{K_f((P_c - Pi)}_{g_1(x_1)} - \underbrace{((\pi_p - \pi_i)) + f2(x_2))}_{g_2(x_2)} - u\end{aligned} \tag{18}$$

Thus

$$\begin{aligned}\dot{x}_1 &= -\, g_1(x_1) + g_2(x_2) - u \\ \dot{x}_2 &= g_1(x_1) - g_2(x_2)\end{aligned} \tag{19}$$

Table I
MODEL PARAMETERS

Parameter	Value	Parameter-Unit	Value
a	0.0065	K_f [L/min*mmHg]	0.0052
b	-146.3	$m_p[g]$	210
c	-54.72	$m_i[g]$	210
d	0.01	P_{off} [mmHg]	13
e	-30.0	k_1	0.21
f	1.5	k_2	0.0016
g	0.02	k_3	9e-6
h	0.63	-	-
i	0.02	-	-

Table II
MODEL VOLUMES

Parameter	Unit	Value-Euhydrated State
$V_{P,eu}$	L	3
$V_{i,eu}$	L	12
V_{rbc}	L	2

C. Theorem 1

We have this Lyapunov function:

$$V(x) = -\frac{1}{2} f(x)^T A f(x)$$

We substitute Q and $f(x)$ in $V(x)$ and simplify the result as

$$\begin{aligned}V(x) =& \frac{1}{2}\{a_{11}f_1(x_1)^2 + a_{22}f_2(x_2)^2 + \ldots + a_{nn}f_n(x_n)^2\} \\ &- 2\{a_{12}f_1(x_1)f_2(x_2) + \ldots + a_{1n}f_1(x_1)f_n(x_n)\} \\ &- 2\{a_{23}f_2(x_2)f_3(x_3) + \ldots + a_{2n}f_2(x_2)f_n(x_n)\} \\ &- 2\{a_{34}f_3(x_3)f_4(x_4) + \ldots + a_{3n}f_3(x_3)f_n(x_n)\} \\ &\ldots - 2\{a_{n-1n}f_{n-1}(x_{n-1})f_n(x_n)\} \\ V(x) =& \frac{1}{2}\left(\sum_{i=1}^{n} f_i(x_i)^2 - 2\sum_{i=1}^{n-1}\sum_{j=i+1}^{n} f_i(x_i)f_j(x_j)\right)\end{aligned}$$

The derivative $\dot{V}(x)$:

$$\begin{aligned}\dot{V}(x) =& \{a_{11}f_1(x_1) - a_{12}f_2(x_2) - a_{13}f_3(x_3) - \ldots \\ &- a_{1n}f_n(x_n)\}\frac{\partial f_1(x)}{\partial x_1}\dot{x}_1 + \{-a_{21}f(x_1) \\ &+ a_{22}f_2(x_2) - \ldots - a_{2n}f_n(x_n)\}\frac{\partial f_2(x)}{\partial x_2}\dot{x}_2 \\ &+ \{-a_{31}f_1(x_1) - a_{32}f_2(x_2) + a_{33}f_3(x_3) \\ &- \ldots - a_{3n}f_n(x_n)\}\frac{\partial f_3(x)}{\partial x_3}\dot{x}_3 + \ldots \\ &\vdots \\ &+ \{-a_{n1}f_1(x_1) - a_{n2}f_2(x_2) + \ldots \\ &+ a_{nn}f_n(x_n)\}\frac{\partial f_n(x)}{\partial x_n}\dot{x}_n \text{ which yields to} \\ =& \{a_{11}f_1(x_1) - \sum_{j\neq i} a_{ij}f_j(x_j(t))\}\frac{\partial f_1(x)}{\partial x_1}\dot{x}_1 \\ &+ \{a_{22}f_2(x_2) - \sum_{j\neq i} a_{ij}f_j(x_j(t))\}\frac{\partial f_2(x)}{\partial x_2}\dot{x}_2 \\ &\vdots \\ &+ \{a_{nn}f_n(x_n) - \sum_{j\neq i} a_{ij}f_j(x_j(t))\}\frac{\partial f_n(x)}{\partial x_n}\dot{x}_n \\ &\text{where } a_{11}f_1(x_1) - \sum_{j\neq i} a_{ij}f_j(x_j(t)) = -\dot{x}_1, \\ &a_{22}f_2(x_2) - \sum_{j\neq i} a_{ij}f_j(x_j(t)) = -\dot{x}_2, \\ &\vdots \\ &a_{nn}f_n(x_n) - \sum_{j\neq i} a_{ij}f_j(x_j(t)) = -\dot{x}_n. \text{ Thus} \\ =& -\dot{x}_1^2\frac{\partial f_1(x)}{\partial x_1} - \dot{x}_2^2\frac{\partial f_2(x)}{\partial x_2} + \ldots - \dot{x}_n^2\frac{\partial f_n(x)}{\partial x_n} \\ \dot{V}(x) =& -\sum_{i=1}^{n}\dot{x}_i^2\frac{\partial f_i(x_i)}{\partial x_i}.\end{aligned}$$

D. Partial Derivative of the Flow

The partial derivative terms: $\frac{\partial \hat{f}_i(x)}{\partial x_i}$, $i = 1, 2$ are derived here:

- $\frac{\partial \hat{f}_1(x_1)}{\partial x_1} = \{\frac{K_f df100}{V_{rbc}+V_{P,eu}}\left(100\frac{V_{rbc}+x_1(t)}{V_{rbc}+V_{P,eu}} + e\right)^{l-1} + K_f\left(\frac{k_1 m_p}{x_1^2(t)} + \frac{k_2 m_p}{x_1^3(t)} + \frac{k_3 m_p}{x_1^4(t)}\right)\} > 0$

- $\frac{\partial \hat{f}_2(x_2)}{\partial x_2} = \Big(K_f \Big\{ \Big(\frac{k_1 m_i}{x_2^2(t)} + \frac{k_2 m_i}{x_2^3(t)} + \frac{k_3 m_i}{x_2^4(t)} \Big) \Big\} + \Big\{ \Big(\frac{100}{V_{i,eu}} (a - \frac{b}{(100 \frac{x_2(t)}{V_{i,eu}} + c)}) \Big) + gsech^2 \Big(ha(100 \frac{x_2(t)}{V_{i,eu}}) + \frac{hb}{(100 \frac{x_2(t)}{V_{i,eu}} + c)} \Big) \times \Big(\frac{h100}{V_{i,eu}} (a - \frac{b}{(100 \frac{x_2(t)}{V_{i,eu}} + c)} \Big) \Big\} \Big) > 0$

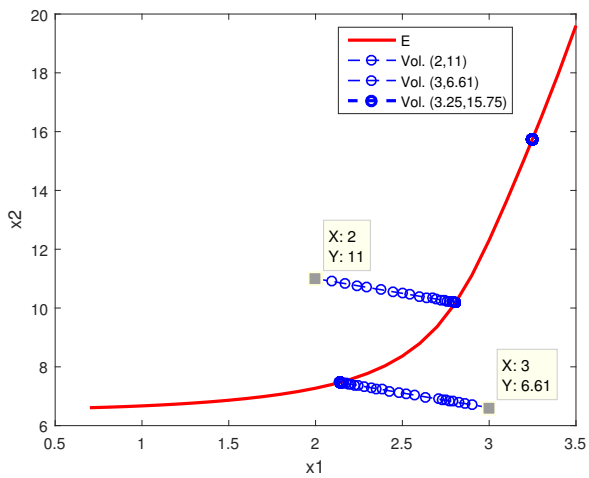

Figure 3. Simulation results show the convergence of the fluid volumes started in three different locations, when the time approaches the infinity, they converge to arbitrary values on E with slope equal to 1.

E. Theorem2

Using $Q(x) = -g_1(x_1) + g_2(x_2)$, it gives

$$\begin{aligned} \dot{x_1} &= Q(x) - u \\ \dot{x_2} &= -Q(x) \end{aligned} \tag{20}$$

and then

$$E := \{x : Q(x) = 0\}.$$

Proof: Along the solution to (5), $\dot{Q}$ is given by

$$\begin{aligned} \dot{Q} &= (Q_{x_1}\dot{x}_1 + Q_{x_2}\dot{x}_2) \\ &= (Q_{x_1}(Q - u) + Q_{x_2}(-Q)) \\ &= (Q_{x_1} - Q_{x_2})Q - Q_{x_1}u(t) \end{aligned} \tag{21}$$

a) At $Q(x) = 0$, from (21) and condition (1), $\dot{Q} = -Q_{x_1}u(t)$:

$$\dot{Q} = \begin{cases} -Q_{x_1}u_{max} > 0, & 0 < t \leq t^* \\ -Q_{x_1}\hat{u}(t) \geq 0 & t^* < t \leq t_f. \end{cases} \tag{22}$$

b) Using $Q(x) = u_{max}$, from (21) and condition (2) $\dot{Q} = Q_{x_1}(u_{max} - u(t)) - Q_{x_2}u_{max}$:

$$\dot{Q} = \begin{cases} -Q_{x_2}u_{max} < 0, & 0 < t \leq t^* \\ (Q_{x_1}(u_{max} - \hat{u}(t)) - Q_{x_2 u_{max}}) < 0 & t^* < t \leq t_f. \end{cases} \tag{23}$$

c) Using $Q(x) \leq u_{max}$, it follows:

$$\begin{aligned} Q(x) - u(t) &\leq u_{max} - u(t) \\ \dot{x}_1 &\leq u_{max} - u(t) \\ x_1 &\leq x_{10} - \int_{\hat{u}(t^*)}^{\hat{u}(t)} \hat{u}(s)ds \\ &\leq x_{10} \end{aligned} \tag{24}$$

d) and using $Q(x) \geq 0$, it follows:

$$\begin{aligned} -Q(x) &\leq 0 \\ \dot{x}_2 &\leq 0 \\ x_2(t) &\leq x_{20} \end{aligned} \tag{25}$$

From (5), we have

$$\dot{x}_1 + \dot{x}_2 = -u(t)$$

then

$$\begin{aligned} x_1 + x_2 &= (x10 + x20) - (u_{max}t + \int_{\hat{u}(t^*)}^{\hat{u}(t)} \hat{u}(s)ds) \\ &> (x10 + x20) - (u_{max}t^* + \int_{\hat{u}(t^*)}^{\hat{u}(t)} \hat{u}(s)ds) \end{aligned}$$

then from a, b, and d: $x(t) \in S$, for all $0 \leq t \leq t_f$. This proves the Theorem. ■

References

[1] Rammah Abohtyra, Yossi Chait, Michael J Germain, Christopher V Hollot, and Joseph Horowitz. Individualization of ultrafiltration in hemodialysis. *IEEE Transactions on Biomedical Engineering*, 66(8):2174–2181, 2018.

[2] A Aurelio, Doris H Fuertinger, Franz Kappel, Anna Meyring-Wösten, Stephan Thijssen, and Peter Kotanko. A physiologically based model of vascular refilling during ultrafiltration in hemodialysis. *Journal of theoretical biology*, 390:146–155, 2016.

[3] Reginald F Brown. Compartmental system analysis: State of the art. *IEEE Transactions on Biomedical Engineering*, (1):1–11, 1980.

[4] PW Chamney, C Johner, C Aldridge, M Kramer, N Valasco, JE Tattersall, T Aukaidey, R Gordon, and RN Greenwood. Fluid balance modelling in patients with kidney failure. *Journal of medical engineering & technology*, 23(2):45–52, 1999.

[5] Airlie Chapman and Mehran Mesbahi. Stability analysis of nonlinear networks via m-matrix theory: Beyond linear consensus. In *2012 American Control Conference (ACC)*, pages 6626–6631. IEEE, 2012.

[6] Sarah Faubel and Joel Topf. *The fluid, electrolyte & acid-base companion*. Alert and Oriented Pub., 1999.

[7] Jurgen Floege, Richard J Johnson, and John Feehally. *Comprehensive clinical nephrology*. Elsevier Health Sciences, 2010.

[8] Jennifer E Flythe, Matthew J Tugman, Julia H Narendra, Magdalene M Assimon, Quefeng Li, Yueting Wang, Steven M Brunelli, and Alan L Hinderliter. Effect of ultrafiltration profiling on outcomes among maintenance hemodialysis patients: a pilot randomized crossover trial. *Journal of Nephrology*, pages 1–11, 2020.

[9] Aimee Stasia Goncalves. Model-based feedback control for hemodialysis treatment of chronic kidney disease patients, 2015.

[10] AC Guyton and JE Hall. Textbook of medical physiology (9th edn) wb saunders company. *Philadelphia. Pennsylvania*, page 1006, 1996.

[11] Arthur C Guyton and JE Hall. The body fluid compartments: extracellular and intracellular fluids; interstitial fluid and edema. *Textbook of medical physiology*, 11:293, 2000.

[12] Wassim M Haddad, Tomohisa Hayakawa, and James M Bailey. Adaptive control for non-negative and compartmental dynamical systems with applications to general anesthesia. *International journal of adaptive control and signal processing*, 17(3):209–235, 2003.

[13] John E Hall. *Pocket companion to Guyton & Hall textbook of medical physiology*. Elsevier Health Sciences, 2015.

[14] John A Jacquez and Carl P Simon. Qualitative theory of compartmental systems. *Siam Review*, 35(1):43–79, 1993.

[15] PR Keshaviah, KM Ilstrup, and FL Shapiro. Dynamics of vascular refilling. *Artif. Organs*, 2:506–10, 1983.

[16] Hassan K Khalil and JW Grizzle. *Nonlinear systems*, volume 3. Prentice hall New Jersey, 1996.

[17] EM Landis and JR Pappenheimer. Exchange of substances through the capillary walls. *Handbook of physiology*, 2(2):961–1034, 1963.

[18] Jing Lin, Zhen Cheng, Xiaoqiang Ding, and Qi Qian. Acid-base and electrolyte managements in chronic kidney disease and end-stage renal disease: Case-based discussion. *Blood purification*, 45(1-3):179–186, 2018.

[19] Hajime Maeda and Shinzo Kodama. Qualitative analysis of a class of nonlinear compartmental systems: nonoscillation and asymptotic stability. *Mathematical Biosciences*, 38(1):35–44, 1978.

[20] Hajime Maeda, Shinzo Kodama, and Yuzo Ohta. Asymptotic behavior of nonlinear compartmental systems: nonoscillation and stability. *Circuits and Systems, IEEE Transactions on*, 25(6):372–378, 1978.

[21] Stefano Marano, Marco Marano, and Leandro Pecchia. Frontiers in hemodialysis part ii: Toward personalized and optimized therapy. *Biomedical Signal Processing and Control*, 61:102029, 2020.

[22] Susumu Ookawara, Kiyonori Ito, Takayuki Uchida, Keito Tokuyama, Satoshi Kiryu, Takeshi Suganuma, Kyoko Hojyo, Haruhisa Miyazawa, Yuichiro Ueda, Chiharu Ito, et al. Hemodialysis crossover study using a relative blood volume change-guided ultrafiltration control compared with standard hemodialysis: the bv-ufc study. *Renal Replacement Therapy*, 6(1):1–10, 2020.

[23] Biff F Palmer and William L Henrich. Recent advances in the prevention and management of intradialytic hypotension. *Journal of the American Society of Nephrology*, 19(1):8–11, 2008.

[24] Donal N Reddan, Lynda Anne Szczech, Vic Hasselblad, Edmund G Lowrie, Robert M Lindsay, Jonathan Himmelfarb, Robert D Toto, John Stivelman, James F Winchester, Linda A Zillman, et al. Intradialytic blood volume monitoring in ambulatory hemodialysis patients: a randomized trial. *Journal of the American Society of Nephrology*, 16(7):2162–2169, 2005.

[25] Patrick B Reeves and Finnian R Mc Causland. Mechanisms, clinical implications, and treatment of intradialytic hypotension. *Clinical journal of the American Society of Nephrology*, 13(8):1297–1303, 2018.

[26] John A Sargent, Marco Marano, Stefano Marano, and F John Gennari. Acid-base homeostasis during hemodialysis: New insights into the mystery of bicarbonate disappearance during treatment. In *Seminars in dialysis*, volume 31, pages 468–478. Wiley Online Library, 2018.

[27] Daniel Schneditz, Johannes Roob, Martina Oswald, Helmuth Pogglitsch, Maximilian Moser, Thomas Kenner, and Ulrich Binswanger. Nature and rate of vascular refilling during hemodialysis and ultrafiltration. *Kidney international*, 42(6):1425–1433, 1992.

[28] Kaoru Tabei, Hirofumi Nagashima, Osamu Imura, Toshihiro Sakurai, and Yasushi Asano. An index of plasma refilling in hemodialysis patients. *Nephron*, 74(2):266–274, 1996.

[29] Mathukumalli Vidyasagar. *Nonlinear systems analysis*, volume 42. Siam, 2002.